Engineering Structures 260 (2022) 114205

Contents lists available at ScienceDirect

Engineering Structures

journal homepage: www.elsevier.com/locate/engstruct

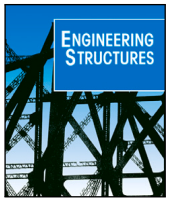

Analysis of torsionally loaded non-uniform circular piles in multi-layered non-homogeneous elastic soils

Carlos A. Vega-Posada [a,*], Mauricio Areiza-Hurtado [b]

[a] Department of Civil and Environmental Engineering, School of Engineering, Univ. de Antioquia, Calle 67 # 53-108. A. A. 1226 Medellín, Colombia
[b] Facultad de Ingenieria, Institucion Universitaria Pascual Bravo, Calle 73 # 73A-226, A. A. 6564 Medellín, Colombia

ARTICLE INFO

Keywords:
Piles & piling
Soil/structure interaction
Foundations
Mathematical modeling
Matrix analysis
Torsion
Multi-layered soil

ABSTRACT

A new method for the torsional analysis of non-uniform circular piles partially or fully embedded in multi-layered elastic soils is developed. The mechanical response of non-uniform piles such as those with a linear variation in cross-section (i.e., tapered piles) or discontinuous variations (i.e., stepped piles), and reacting against a non-homogeneous elastic soil can be easily investigated with the proposed formulation. The non-homogeneity of the soil is incorporated by assuming a shear modulus distribution that fits a quadratic equation (i.e., $G(z) = G_o + sz + tz^2$). The governing differential equation (GDE) of a single non-uniform circular pile segment is derived and solved using the differential transformation method (DTM); then, the stiffness matrix of the segment is found by applying equilibrium and compatibility conditions at the ends of the element. The analysis of non-uniform piles in multi-layered soils is conducted by dividing the pile into multiple segments (i.e., each segment representing a change in soil properties or pile geometry) and then assembling them using classic matrix methods. The proposed matrix formulation is simple to implement, easy to incorporate into already available structural matrix analysis codes and provides accurate results when compared with more cumbersome analytical and numerical solutions. The simplicity, practicality and accuracy of the method is validated with five illustrative examples.

1. Introduction

Non-uniform cross-section piles such as tapered and stepped piles are commonly used in many geotechnical applications because they provide higher compressive axial, lateral and torsional capacities than cylindrical piles [1–6]. Thus, because of the taper angle, they also provide a more efficient drivability performance during construction [7,8]. Piles are usually designed to resist large lateral and torsional loads such as those resulting from accidental collisions, environmental loads (i.e., wind and wave loads in offshore structures), earthquake-induced loads, lateral soil movement loads, etc. The superiority in capacity of tapered and stepped piles over cylindrical ones of the same length and volume are due to the larger cross-sectional area at the upper portion of the pile (i.e., higher stiffness).

Many researchers have investigated the torsional performance of piles via analytical- or numerical-based techniques [9–18]. Most of these methods are limited to piles with a uniform cross-section (i.e., prismatic piles), embedded in a single- or double-layered soil and with a constant or linear distribution of the shear modulus. From these studies, and because of the complexity of the analysis, only very few of them have been devoted to investigate piles with non-uniform sections [19,20]. Even though piles are commonly embedded in soils made up of multiple layers, and each layer has it own properties, available analytical methods accounting for this fact are rather limited [21,22], and even more limited for piles with non-uniform cross-sections. Moreover, these methods are mathematically very complicated, requiring, in most cases, calculus of variations schemes and iterative procedures to find the solution. A technical literature review indicates that the analysis of torsional loaded non-uniform piles in multi-layered soils has received little attention, and that there is still a lack of simple, analytical approaches to conduct these types of analyses.

This paper presents a new, simple analytical approach to investigate the mechanical response of non-uniform circular piles (i.e., tapered piles, stepped piles, etc.) in multi-layered non-homogeneous soils and subjected to torsional loads. This research is a continuation of a work previously presented by the first author to analyze prismatic piles [23] and now is extended to investigate the torsional response of non-uniform circular piles. The approach is limited to piles in elastic soils and slippage at the soil–pile interface is neglected. The governing

* Corresponding author.
E-mail address: carlosa.vega@udea.edu.co (C.A. Vega-Posada).

https://doi.org/10.1016/j.engstruct.2022.114205
Received 19 November 2021; Received in revised form 28 February 2022; Accepted 26 March 2022
Available online 12 April 2022

differential equation (GDE) of a segment of pile is derived in a classical manner and solved using the Differential Transformation Method (DTM). The distribution of the shear modulus along the pile segment is assumed to fit a quadratic function, so a wide range of soil conditions can be accounted for. Simple steps are provided to study the torsional response (i.e., variation of the angle of twist with depth) of piles in a single-layered soil while accounting for the contribution of the torsional stiffness at the pile base. The exact solution of a segment is used to derive the segment's stiffness matrix by applying compatibility conditions at the ends of the element. The analysis of piles in multi-layered soils is carried out by (i) dividing the pile into multiple segments; one segment assigned to each portion of the pile with different soil properties or geometry conditions, (ii) computing the stiffness matrix of each segment and then (iii) assembling the global stiffness matrix of the entire pile by means of convention matrix methods. In this manner, the torsional response of the entire pile can be investigated. In addition to fully embedded piles, and because of the advantages of the matrix formulation, partially embedded piles can also be studied by simply neglecting the contribution of the soil in the unembedded portion. The proposed formulation can be easily integrated into already available matrix structural analysis codes.

2. Formulation of problem

Fig. 1 shows the main features of the formulated problem. Fig. 1(a) depicts a prismatic, tapered and stepped pile subjected to a torque T at the pile head and embedded in a soil with ith layers. The pile segment has a shear modulus Gp, variable polar moment of inertia $J(z)$, variable cross-sectional area $A(z)$ and length L_p. For the analysis, the pile is subdivided into a number of segments, one segment for every change in soil properties or pile geometry. Fig. 1(b) shows a segment of pile of length L (i.e., segment AB - layer 3) for which the constitutive GDE and stiffness matrix are derived. The soil is modeled with rotational discrete springs, and the shear modulus within each layer is assumed to vary with depth following a quadratic function of the form $G(z) = G_o+sz+tz^2$ (Fig. 1(c)). $s = t = 0$ represents a homogeneous distribution of $G(z)$ and $t = 0$ a linear increasing or decreasing variation of $G(z)$. The soil is represented as a discrete, independent linear elastic spring. This simplification is analogous to the well-known soil model proposed by Winkler for a beam resting on elastic foundation. Discrete methods are simple to implement and, as shown by many researchers, they accurately predict the torsional response of piles [12,18,22]. Fig. 2 shows a reference circular pile for the tapered elements. Here, r_b and r_t are the radius at the top and bottom of the pile, respectively. r_{eq} is the radius at $z = L_p/2$. m is the taper ratio and is defined as $m = r_b/r_t$. $m = 1$ correspond to a prismatic pile.

It is assumed that the pile: (i) twists about its principal longitudinal axis; (ii) behaves as a homogeneous, isotropic, linear elastic material and (iii) experiences only St. Venant torsion stresses. These assumptions are considered appropriate from a practical perspective, where the design engineer limits the magnitude of the torsional load that the foundation will experience and both the soil and pile element remain in the linear regime for the applied loads (working loads), factors of safety implemented for design and torsional rotation design limitations. Next, the governing differential equation (GDE) of a single pile segment, its corresponding analytical solution and the derivation of its stiffness matrix – a required step to investigate piles in multi-layered soils – are presented.

3. Governing equations

The GDE of the solid circular tapered pile subjected to torsional loads and embedded in a non-homogeneous elastic media (i.e., segment AB shown in Fig. 1(b)) can be expressed as [15,16]:

$$\frac{d}{dz}\left[G_p J(z)\frac{d\theta}{dz}\right] = 2\pi r^2(z)\tau(z) \tag{1}$$

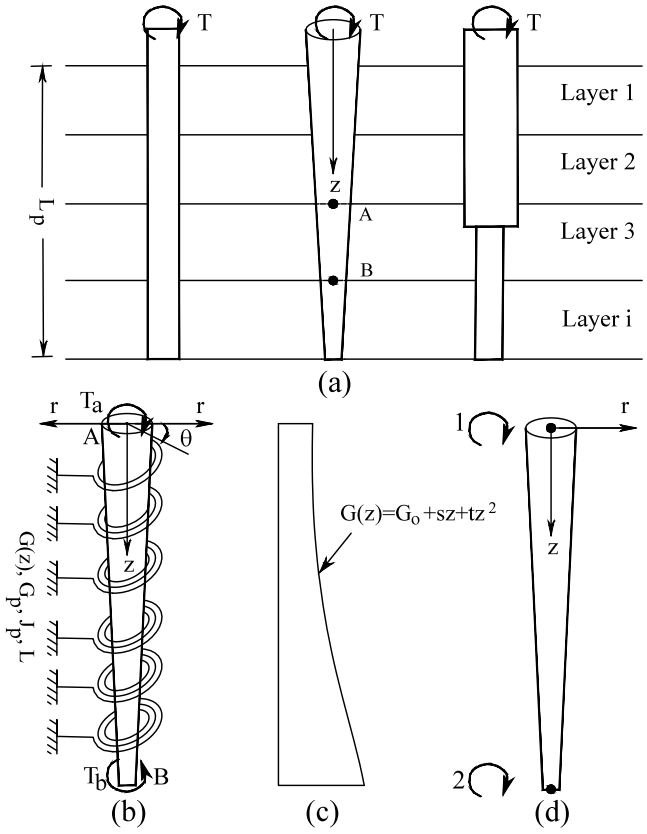

Fig. 1. (a) Non-uniform piles in a multi-layered soil; (b) single pile segment (structural model); (c) shear modulus distribution along a pile segment and (d) local degrees of freedom and right hand sign convention for torques and rotations.

where $\tau(z) = 2G(z)\theta(z)$ for elastic conditions. $\tau(z)$ and $\theta(z)$ are, respectively, the shear stress at the soil–pile interface and angle of twist at a depth z. $r(z)$ and $J(z)$ are the pile's radius and polar moment of inertia at a depth z, respectively. They are given by:

$$r(z) = r_t\left[1 + \frac{z}{L}(m-1)\right] \tag{2}$$

$$J(z) = \frac{\pi}{2}r^4(z) = \frac{\pi}{2}r_t^4\left[1 + \frac{z}{L}(m-1)\right]^4 \tag{3}$$

Now, substituting $r(z)$ and $G(z)$ into Eq. (1), the following expression for the GDE is obtained:

$$\frac{d}{dz}\left[G_p J(z)\frac{d\theta}{dz}\right] = 4\pi\left\{r_t\left[1 + \frac{z}{L}(m-1)\right]\right\}^2(G_o + sz + tz^2)\theta(z) \tag{4}$$

For analysis of one single element (i.e., segment AB), $z = 0$ corresponds to end A of the element and $z = L$ to end B. Introducing the normalized variable $\zeta = z/L$, and expanding the first term in Eq. (4), the GDE becomes:

$$\frac{G_p J(\zeta)}{L^2}\frac{d^2\theta}{d\zeta^2} + \frac{G_p}{L^2}\frac{d\theta}{d\zeta}\frac{dJ}{d\zeta} = R(\zeta)\theta(\zeta) \tag{5}$$

Recall that $d^n/dx^n = (1/L)^n(d^n/d\zeta^n)$. Eq. (5) is the normalized second order DE that governs the torsional response of the proposed structural segment. Here, $R(\zeta) = R_0 + R_1\zeta + R_2\zeta^2 + R_3\zeta^3 + R_4\zeta^4$ and $J(\zeta) = S_0 + S_1\zeta + S_2\zeta^2 + S_3\zeta^3 + S_4\zeta^4$. Table 1 lists the expressions for terms comprising functions $R(\zeta)$ and $J(\zeta)$.

The Differential Transformation Method (DTM) is used to solve the GDE. The DTM transforms, in an easy and rather elegant manner, the GDE into a recurrence equation and the boundary conditions (B.Cs.) into algebraic expressions. Thus, the solution to this complex DE (Eq. (5)) is reduced to solve a simple linear algebraic equation. The

Table 1
Expressions for terms comprising functions $R(\zeta)$ and $J(\zeta)$.

$R(\zeta)$ and $J(\zeta)$
$R_0 = 4\pi r_t^2 \cdot G_o$
$R_1 = 4\pi r_t^2 \cdot [2(m-1)G_o + sL]$
$R_2 = 4\pi r_t^2 \cdot [nL^2 + 2(m-1)sL + (m-1)^2 G_o]$
$R_3 = 4\pi r_t^2 \cdot [2(m-1)tL^2 + (m-1)^2 sL]$
$R_4 = 4\pi r_t^2 \cdot [(m-1)^2 tL^2]$
$S_0 = \pi r_t^4/2$
$S_1 = 4\pi r_t^4/2 \cdot (m-1)$
$S_2 = 6\pi r_t^4/2 \cdot (m-1)^2$
$S_3 = 4\pi r_t^4/2 \cdot (m-1)^3$
$S_4 = \pi r_t^4/2 \cdot (m-1)^4$

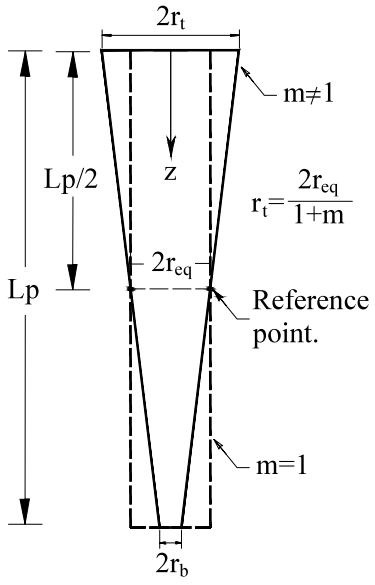

Fig. 2. Reference circular tapered pile.

main properties of the DTM are listed in Table 2. For further details about the DTM method the reader is referred to [24–26].

The angle of twist is expressed in terms of the DTM method as follows:

$$\theta(\zeta) = \bar{\theta}(0) + \bar{\theta}(1)\zeta + \bar{\theta}(2)\zeta^2 + \bar{\theta}(3)\zeta^3 + \cdots + \bar{\theta}(i)\zeta^i = \sum_{k=0}^{\infty} \bar{\theta}(k)\zeta^k \tag{6}$$

and

$$\bar{\theta}(k) = \frac{1}{k!}\left[\frac{d^k\theta(\zeta)}{d\zeta^k}\right]_{\zeta=0} \tag{7}$$

where $\theta(\zeta)$ is the angle of twist and $\bar{\theta}(k)$ is the transformed of the kth derivative of $\theta(\zeta)$ [24]. Term i of the series is selected such that the contribution of the next term (i.e., $\bar{\theta}(i+1)\xi^{i+1}$) is less than an arbitrary small number (i.e., for instance, $\epsilon < 10^{-6}$). Now, using the properties of the DTM listed in Table 2, Eq. (5) can be expressed in a recurrence form as follows (see Appendix):

$$\begin{aligned}\bar{\theta}(k+2) = &\left\{ \frac{L^2}{G_p}\left[R_o\bar{\theta}(k) + R_1\bar{\theta}(k-1) + R_2\bar{\theta}(k-2) + R_3\bar{\theta}(k-3) \right.\right.\\ &\left. + R_4\bar{\theta}(k-4)\right]\\ &- \left[S_1(k+1)^2\bar{\theta}(k+1) + S_2k(k+1)\bar{\theta}(k) + S_3(k-1)(k+1)\bar{\theta}(k-1) \right.\\ &\left.\left. + S_4(k-2)(k+1)\bar{\theta}(k-2)\right]\right\} / \left\{ S_0(k+1)(k+2) \right\}\end{aligned} \tag{8}$$

Table 2
DTM properties.

	Original function	Transformed function
1	$y(\zeta) = g(\zeta) \pm h(\zeta)$	$\bar{Y}(k) = \bar{G}(k) \pm \bar{H}(k)$
2	$y(x) = \alpha g(\zeta)$	$\bar{Y}(k) = \alpha\bar{G}(k)$
3	$y(\zeta) = \frac{d^n g(\zeta)}{d\zeta^n}$	$\bar{Y}(k) = \frac{(k+n)!}{k!}\bar{G}(k+n)$
4	$y(\zeta) = g(\zeta)h(\zeta)$	$\bar{Y}(k) = \sum_{r=0}^{k}\bar{G}(r)\bar{H}(k-r)$
5	$y(\zeta) = \zeta^n$ (*)	$\bar{Y}(k) = \delta(k-n) = \begin{cases} 0 & \text{if } k \neq n \\ 1 & \text{if } k = n \end{cases}$

Eq. (8) is the GDE transformed into a recurrence equation and is used to determine coefficients $\bar{\theta}(k)$ of the proposed solution (Eq. (6)). Here, $\bar{\theta}(-1) = \bar{\theta}(-2) = \bar{\theta}(-3) = \bar{\theta}(-4) = 0$. Coefficients $\bar{\theta}(0)$ and $\bar{\theta}(1)$ are found from the B.Cs. at $\zeta = 0$. Coefficients $\bar{\theta}(2) - \bar{\theta}(i)$ are linear combinations of $\bar{\theta}(0)$ and $\bar{\theta}(1)$.

The B.Cs. at ends AB of the pile segment are:

At $\zeta = 0$:

$$\frac{d\theta}{d\zeta} \mid_{\zeta=0} = -T_a L/(G_p J o) = \bar{\theta}(1) \tag{9}$$

At $\zeta = 1$:

$$\frac{d\theta}{d\zeta} \mid_{\zeta=1} = -T_b L/(G_p J_1) = \sum_{k=0}^{\infty} k\bar{\theta}(k) \tag{10}$$

where T_a and T_b are the torques at ends A and B of the element and J_0 and J_1 are the polar moment of inertia evaluated at $z = 0$ and $z = L$, respectively (from Eq. (3)). At the pile base, the relation between the torque and twist is given by [27]:

$$\theta \mid_{\zeta=1} = \sum_{k=0}^{\infty}\bar{\theta}(k) = \frac{3}{16}\cdot\frac{T_b}{G_b r_b^3} \tag{11}$$

where G_b is the shear modulus at the base of the pile. Substituting Eq. (11) into Eq. (10), the following expression at the pile base is found:

$$-\frac{16}{3}G_b r_b^3 \frac{L}{G_p J_1}\sum_{k=0}^{\infty}\bar{\theta}(k) = \sum_{k=0}^{\infty} k\bar{\theta}(k) \tag{12}$$

4. Proposed solution

The solution to Eq. (6) consists of finding coefficients $\bar{\theta}(k)$ that satisfy the B.Cs. at ends A and B of the element. The following simple steps are provided:

1. Assume an initial, arbitrary small value of $\bar{\theta}(0)$.
2. Compute $\bar{\theta}(1)$ from Eq. (9).
3. Determine coefficients $\bar{\theta}(2) - \bar{\theta}(i)$ from the recursive equation (Eq. (8)).
4. Solve the following linear algebraic expression (Eq. (12)).

$$F(\bar{\theta}(0)) = \frac{16}{3}G_b r_b^3\sum_{k=0}^{\infty}\bar{\theta}(k) + \frac{G_p J_1}{L}\sum_{k=0}^{\infty} k\bar{\theta}(k) \tag{13}$$

5. Increase in a step-wise fashion the value of $\bar{\theta}(0)$ and repeat steps (1) – (4). Plot $\bar{\theta}(0)$ against $F(\bar{\theta}(0))$.
6. Select coefficient $\bar{\theta}(0)$ that makes $F(\bar{\theta}(0)) = 0$ (i.e., this coefficient satisfies both B.Cs.)
7. Once $\bar{\theta}(0)$ is known, repeat steps (2) and (3) and determine the angle of twist profile from Eq. (6).
8. The torque profile can be found from Eq. (14):

$$T(\zeta) = -\frac{G_p J(\zeta)}{L}\frac{d\theta}{d\zeta} \tag{14}$$

Steps (1)–(8) can be used to study the overall torsional response of single non-uniform circular piles in a one-layered soil profile while accounting for the contribution of the torsional stiffness at the pile base.

As stated by Randolph [27], the contribution of the base quickly becomes insignificant, even for rigid piles, as the length and flexibility of the pile increase. Therefore, for practical applications, and in particular for piles in multi-layered soils, this contribution can be neglected.

5. Stiffness matrix derivation

The local stiffness matrix of the pile segment AB shown in Fig. 1 is derived from equilibrium and compatibility conditions. This matrix relates the nodal torques and angles of twist in local coordinates. The stiffness matrix method is used to analyze non-uniform circular piles in multi-layered soils. Here, the torsional stiffness contribution of the pile base is neglected. For further details about the stiffness matrix method, the reader is referred to Przemieniecki [28] and McGuire et al. [29]. Segment AB could represent a layer of soil in a multi-layered soil profile or a portion of the pile with different material or geometry properties (i.e., stepped piles). The stiffness matrix has a size of 2 x 2, one for each degree of freedom (rotation) at each end of segment AB. Fig. 1(d) shows the right-hand sign convention adopted in the matrix analysis for the torques and rotations.

The angle of twist at $\zeta = 0$ can be evaluated using Eq. (6). At $\zeta = 1$, and taking into account that coefficients $\bar{\theta}(2) - \bar{\theta}(i)$ are linear combinations of $\bar{\theta}(0)$ and $\bar{\theta}(1)$, $\theta(\zeta)$ can be conveniently expressed as:

$$\theta(\zeta = 1) = f_0\bar{\theta}(0) + f_1\bar{\theta}(1) \tag{15}$$

where f_0 and f_1 are functions that grouped the coefficients of the series affected by $\bar{\theta}(0)$ and $\bar{\theta}(1)$, respectively. f_0 is the value of $\theta(\zeta = 1)$ in Eq. (6) when $\bar{\theta}(0) = 1$ and $\bar{\theta}(1) = 0$. Coefficients $\bar{\theta}(2) - \bar{\theta}(i)$ are computed from Eq. (8). f_1 is determined in an analogous manner by taking $\bar{\theta}(0) = 0$ and $\bar{\theta}(1) = 1$. By definition, terms S_{11} and S_{21} of the matrix are the holding actions at ends AB, respectively, when a unit rotation is imposed at node 1 while holding the rotation at node 2 to zero. Terms S_{12} and S_{22} are determined in an analogous manner by imposing a unit rotation at node 2 while holding the rotation at node 1 to zero.

When a unit rotation is imposed at node 1 ($\theta(0) = 1$) while holding the rotation at node 2 to zero ($\theta(1) = 0$), one has:

$$\theta(\zeta) = 1 = \bar{\theta}(0) \tag{16}$$

$$\theta(\zeta) = 0 = f_0\bar{\theta}(0) + f_1\bar{\theta}(1) \tag{17}$$

From Eqs. (16) and (17), $\bar{\theta}(0) = 1$ and $\bar{\theta}(1) = -f_0/f_1$. Terms S_{11} and S_{21} are determined as follows:

$$T(\zeta = 0) = S_{11} = -\frac{G_pJ_0}{L}\frac{d\theta}{d\zeta} \mid_{\zeta=0} = -\frac{G_pJ_0}{L}\bar{\theta}(1) \tag{18}$$

$$= \frac{G_pJ_0}{L}\frac{f_0}{f_1} \tag{19}$$

$$T(\zeta = 1) = S_{21} = \frac{G_pJ_1}{L}\frac{d\theta}{d\zeta} \mid_{\zeta=1} = \frac{G_pJ_1}{L}(f_{01}\bar{\theta}(0) + f_{11}\bar{\theta}(1))$$

$$= \frac{G_pJ_1}{L}\left(f_{01} - \frac{f_0f_{11}}{f_1}\right) \tag{20}$$

Now, when a unit rotation is imposed at node 2 ($\theta(1) = 1$) while holding the rotation at node 1 to zero ($\theta(0) = 0$), one has:

$$\theta(\zeta) = 0 = \bar{\theta}(0) \tag{21}$$

$$\theta(\zeta) = 1 = f_0\bar{\theta}(0) + f_1\bar{\theta}(1) \tag{22}$$

From Eqs. (21) and (22), $\bar{\theta}(0) = 0$ and $\bar{\theta}(1) = 1/f_1$. Terms S_{12} and S_{22} are determined as follows:

$$T(\zeta = 0) = S_{12} = -\frac{G_pJ_0}{L}\frac{d\theta}{d\zeta} \mid_{\zeta=0} = -\frac{G_pJ_0}{L}\bar{\theta}(1) = -\frac{G_pJ_0}{L}\frac{1}{f_1} \tag{23}$$

$$T(\zeta = 1) = S_{22} = \frac{G_pJ_1}{L}\frac{d\theta}{d\zeta} \mid_{\zeta=1} = \frac{G_pJ_1}{L}(f_{01}\bar{\theta}(0) + f_{11}\bar{\theta}(1)) = \frac{G_pJ_1}{L}\frac{f_{11}}{f_1} \tag{24}$$

where f_{01} is the value of $\theta'(\zeta)$ at $\zeta = 1$ (i.e., $\theta'(\zeta) = \sum_{k=0}^{m} k\bar{\theta}(k)$) when $\bar{\theta}(0) = 1$ and $\bar{\theta}(1) = 0$. f_{11} is the value of $\theta'(\zeta)$ at $\zeta = 1$ when $\bar{\theta}(0) = 0$ and $\bar{\theta}(1) = 1$. The stiffness matrix of the segment, matrix $[K]$, can be expressed as follows:

$$[K] = \begin{bmatrix} K_{11} & K_{12} \\ K_{21} & K_{22} \end{bmatrix} = \frac{G_p}{L}\begin{bmatrix} J_0f_0/f_1 & -J_0/f_1 \\ -J_1(f_{11}f_0/f_1) + J_1f_{01} & J_1f_{11}/f_1 \end{bmatrix} \tag{25}$$

6. Verification of the new method

6.1. Example 1: Pile in a one-layered homogeneous soil

Fig. 3 shows the torsional stiffness ratio, $T_{SR} = 3T_o/(16G_br_b^3\theta_o)$, and distribution of the normalized torque, $T(z)/T_o$, for a prismatic ($m = r_b/r_t = 1$) and tapered ($m \neq 1$) pile. Steps (1) to (8) from Section 4 were employed to find the overall torsional response. The pile is subjected to a torsional load T_o at its head and embedded in a one-layered homogeneous elastic soil (i.e., uniform distribution of $G(z)$). The soil has a shear modulus G_o along the pile length and G_b at the pile base. In order to have some means of comparison with already published works, the definition of the taper ratio was modified in this example. Here, the reference point is located at the corner of the pile head as depicted in Fig. 3(a) and not at $L_P/2$ as proposed for the matrix analysis approach (Fig. 2).

Fig. 3(a) shows the torsional stiffness ratio as a function of the soil–pile stiffness ratio, G_p/G_o, for a prismatic pile. G_p is the shear modulus of the pile. The analysis was conducted for three slenderness ratios ($L/r_t = 5, 10$ and 30) and two soil stiffness ratios ($G_b/G_o = 1$ and 10). It is seen that for piles that behave as very flexible piles (i.e., low values of G_p/G_o), T_{SR} was independent of the slenderness ratio regardless of the shear modulus at the pile base. Similar trends have been reported by Poulos [9] and Randolph [10]. Fig. 3(b) shows T_{SR} as a function of L/r_t and m. It is observed that: (i) T_{SR} increased as L/r_t increased due to a decrease in the angle of twist at the pile head (θ_o) associated to the increment in slenderness ratio and (ii) the magnitude of T_{SR} was greater for $m = 0.75$ than for $m = 0.50$ due to a decrease in θ_o associated to a greater cross-section at the upper portion of the segment (i.e., higher pile stiffness). The results are in good agreement with those obtained from the variation scheme and numerical solution developed by Rajapakse and Selvadurai [19] and Selvadurai and Rajapakse [20].

Figs. 3(c) and (d) present the torque distribution profiles for a short pile of length $L = 5r_t$ and a shear modulus at the pile base of $G_b = G_o$ and $G_b = 10G_o$, respectively. The analysis was conducted for $m = 1, 0.75$ and 0.50. It is observed that the torque profile was almost linear for the prismatic pile and slightly concave up for the tapered ones. The portion of the applied torque at a given depth became smaller as the taper ratio decreased. This is because of the reduction in cross-section with depth. Note that the portion of the torque at the pile base corresponds to the value of $T(z)/T_o$ at $z/r_t = 5$. As anticipated, for short piles, the magnitude of the torque transferred at the pile base increased significantly as the G_b/G_o ratio increased, and it was greater for the prismatic pile than for the tapered ones (i.e., because of the bigger cross-section at the pile base).

6.2. Example 2: Tapered pile in a two-layered homogeneous soil

Fig. 4 shows the torsional stiffness factor, $T_t/(G_2r_{eq}^3\theta_t)$, plotted against the length ratio, h/L, for a tapered pile embedded in a two-layered homogeneous elastic soil (i.e., G_1 and G_2 are constant). h and $L-h$ are the thicknesses of the top and bottom layers, respectively, and G_1 and G_2 their corresponding shear modulus. Length ratios $h/L = 0$ and $h/L = 1$ represent a pile in a one-layered soil with constant shear modulus G_2 and G_1, respectively. The analysis was conducted for four shear modulus ratios ($G_1/G_2 = 4, 2, 0.5$ and 0.25) and nine taper ratios ($m = 1, 0.9, 0.8, 0.7, 0.6, 0.5, 0.4, 0.3$ and 0.2). The reference point for parameter m was located at a depth $L_p/2$, as depicted in Fig. 2. The

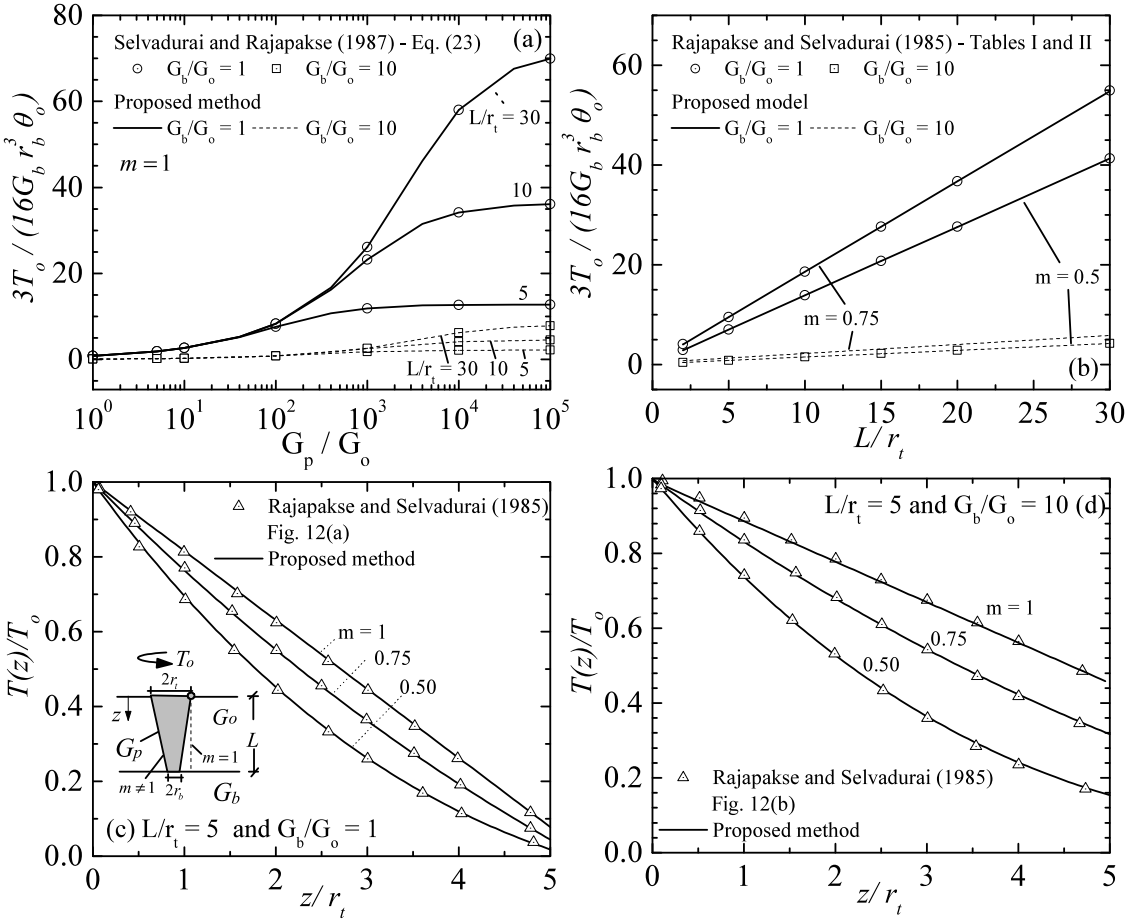

Fig. 3. Example 1: Torsional stiffness and torque distribution of a prismatic and tapered pile in a one-layered soil while accounting for the contribution of the torsional stiffness at the pile base.

following parameters were used for the parametric study: $r_{eq} = 0.5$ m, $L = 25$ m, $G_p = 8$ GPa, $G_2 = 8$ MPa and $T = 100$ kN m.

For the matrix analysis, the pile was subdivided into two segments. Segment 1 was assigned to the portion of the pile embedded in the bottom layer with thickness $L - h$ and shear modulus G_2, and segment 2 to the portion of the pile embedded in the top layer with thickness h and shear modulus G_1. Note that for a given taper ratio (m), the stiffness matrix of each segment must be computed with its local taper ratio, and this value will depend on the length ratio h/L. Fig. 4(d) shows the structural model, segment numbering, and global degrees of freedom at the joints. The overall torsional response of the pile was carried out by computing the individual local stiffness matrix of each segment and then connecting them at the joints by using conventional matrix structural analysis. The global stiffness and joint load matrices of the pile are expressed as:

$$[K_G] = \begin{matrix} 1 & 2 & 3 \end{matrix} \begin{bmatrix} K_{11}^1 & K_{12}^1 & 0 \\ K_{21}^1 & K_{22}^1 + K_{11}^2 & K_{12}^2 \\ 0 & K_{21}^2 & K_{22}^2 \end{bmatrix} \begin{matrix} 1 \\ 2 \\ 3 \end{matrix} \quad ; \quad \{T\} = \begin{Bmatrix} 0 \\ 0 \\ T_t \end{Bmatrix} \begin{matrix} 1 \\ 2 \\ 3 \end{matrix}$$

Here, the numbers outside the brackets indicate the global degrees of freedom at the joints. The superscripts of the matrix coefficients indicate the segment number. For example, K_{12}^1 corresponds to coefficient K_{12} of segment 1. Once the global stiffness matrix and nodal forces are known, the nodal angles of twist can be obtained by solving $\{\theta\} = [K_G]^{-1}\{T\}$. $\{\theta\} = \{\theta_1, \theta_2, \theta_3\}^T$ are the angles of twist at nodes 1, 2 and 3, respectively.

Figs. 4 and 5 show the contribution of both the taper ratio and surrounding soil at the upper portion of the pile on the torsional capacity. Fig. 5 shows the torsional stiffness factor for taper ratios $m = 1, 0.8, 0.5$ and 0.2. For the cases when $G_1/G_2 = 4$ and $G_1/G_2 = 2$, and regardless of the taper ratio, the torsional stiffness factor rapidly increased until the thickness of the top layer was approximately 30% the length of the pile ($h/L > 0.3$) and then it remained constant. The increase in capacity was due to a larger shear modulus along the upper portion of the pile. In an analogous manner, when $G_1/G_2 = 0.5$ and $G_1/G_2 = 0.25$, the torsional stiffness factor gently dropped until h/L was approximately 50% and then it remained constant. From these figures, it is also seen that, irrespective of the G_1/G_2 ratio, the torsional stiffness significantly increased as the taper ratio decreased, highlighting the advantages of tapered piles over conventional prismatic ones in terms of torsional capacity. For prismatic piles ($m = 1$), the results from the proposed model were compared with those reported by Chow [12], Zhang [17] and Zou et al. [18]. For tapered piles ($m \neq 1$), and due to the lack of published works, they were compared with results obtained from the finite element analysis package Abaqus 3D. The agreement between the results from the proposed formulation and those obtained from much more cumbersome analytical and numerical approaches was excellent.

6.3. Example 3: Tapered pile in a four-layered soil

Fig. 6 shows the angle of twist profile for a tapered pile in a four-layered soil subjected to a torsional load of 100 kN m at its head. The analysis is conducted for taper ratios $m = 1, 0.8, 0.5$ and 0.2. The pile has i) a shear modulus $G_p = 9.6 \cdot 10^6$ kPa, (ii) an equivalent radius of 0.5 m

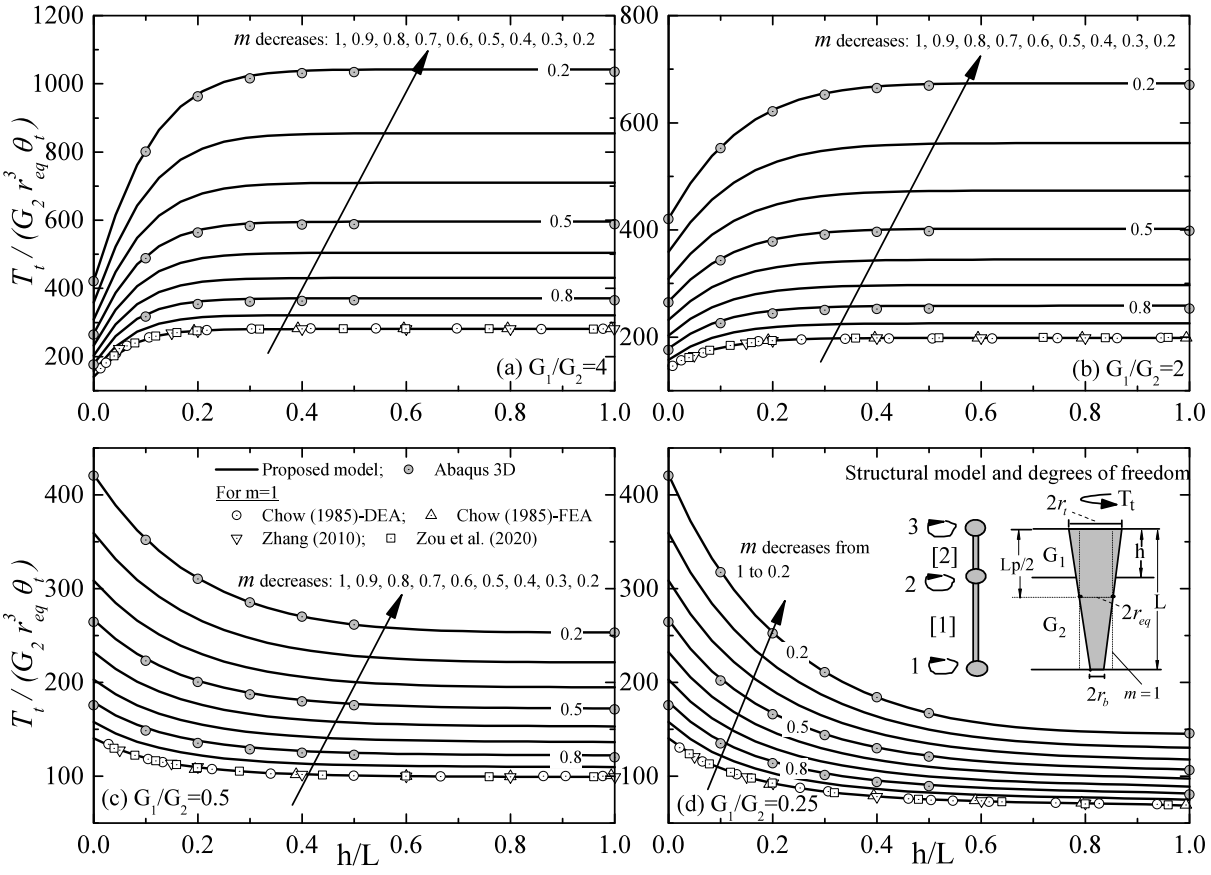

Fig. 4. Example 2: Torsional stiffness factor versus length ratio for a tapered pile in a two-layered homogeneous soil when (a) $G_1/G_2 = 4$, (b) $G_1/G_2 = 2$, (c) $G_1/G_2 = 0.5$ and (d) $G_1/G_2 = 0.25$.

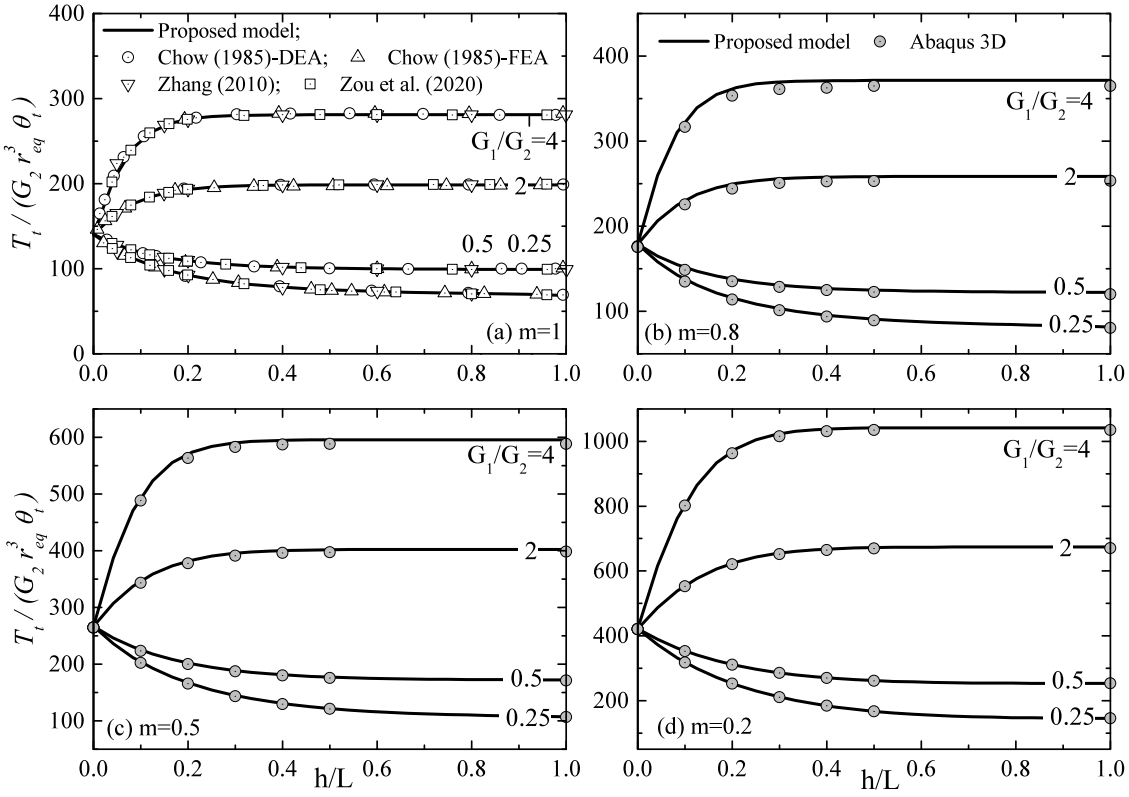

Fig. 5. Example 2: Torsional stiffness factor versus length ratio for a tapered pile in a two-layered homogeneous soil for (a) $m = 1$, (b) $m = 0.8$, (c) $m = 0.5$ and (d) $m = 0.2$.

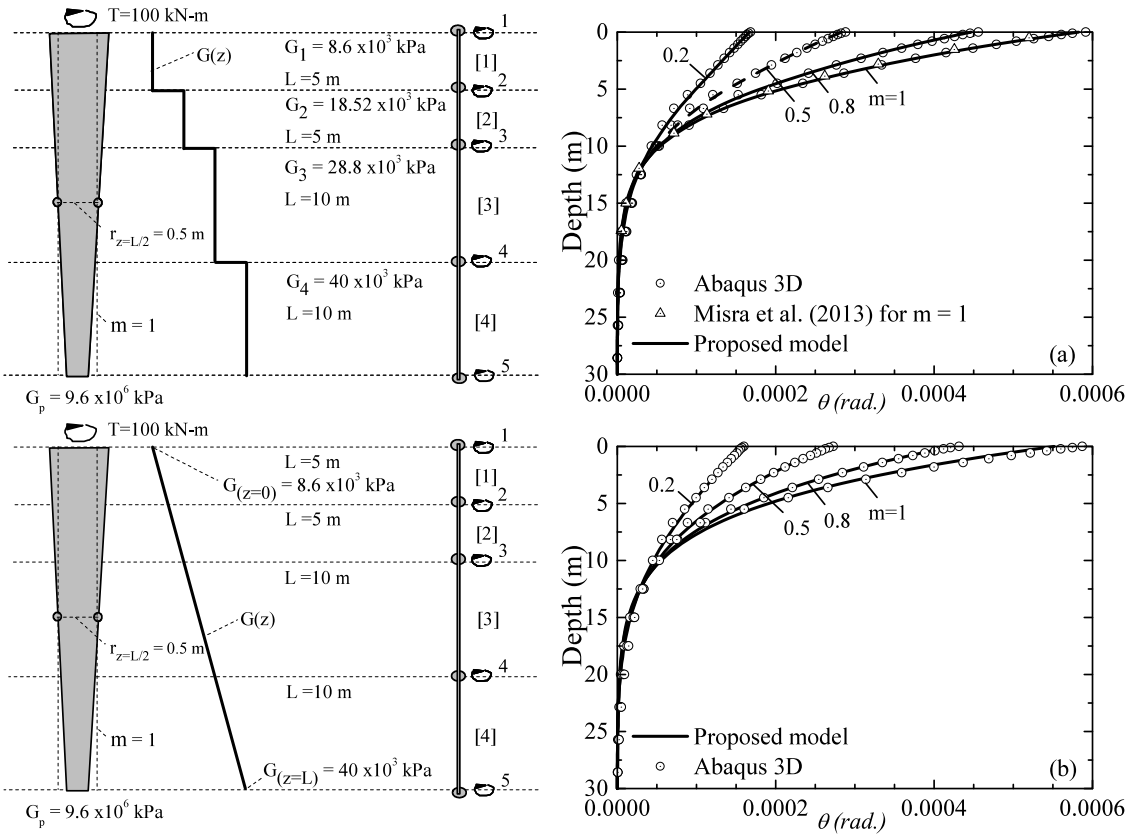

Fig. 6. Example 3: Tapered pile in a four-layered soil: (a) increase of $G(z)$ with depth in a step-wise manner and (b) linear increase distribution of $G(z)$.

(at a depth $L_p/2$) and (iii) a length of 25 m. Two cases are considered in this example. The first case considers a soil where $G(z)$ increases with depth in a step-wise manner, as shown in Fig. 6(a) (i.e., each individual layer has a uniform distribution of G). From top to bottom, the shear modulus G and thickness L of the first three layers are $8.6 \cdot 10^3$ kPa and 5 m, $18.52 \cdot 10^3$ kPa and 5 m, and $28.8 \cdot 10^3$ kPa and 10 m. The fourth layer has a shear modulus of $40 \cdot 10^3$ kPa and extends to a greater depth beyond the toe of the pile. These soil and pile parameters are similar to those previously implemented by Misra et al. [21] for the case of a prismatic pile in a four-layered soil deposit. The second case considers the condition where $G(z)$ increases with depth in a linear fashion, as shown in Fig. 6(b) (i.e., each individual layer has a linear distribution of G). Here, the shear modulus at the surface is $G_{z=0} = 8.6 \cdot 10^3$ kPa and at the pile toe $G_{z=L_p} = 40 \cdot 10^3$ kPa.

The analysis was carried out by subdivided the pile into four segments, one segment for each layer. The elements, degrees of freedom and their numbering are shown in Fig. 6. The global stiffness and joint load matrices of the entire pile are expressed in a symbolic form as follows:

$$[K_G] = \begin{matrix} \\ 1 \\ 2 \\ 3 \\ 4 \\ 5 \end{matrix} \begin{matrix} \begin{matrix} 1 & 2 & 3 & 4 & 5 \end{matrix} \\ \begin{bmatrix} K_{11}^1 & K_{12}^1 & 0 & 0 & 0 \\ K_{21}^1 & K_{22}^1 + K_{11}^2 & K_{12}^2 & 0 & 0 \\ 0 & K_{21}^2 & K_{22}^2 + K_{11}^3 & K_{12}^3 & 0 \\ 0 & 0 & K_{21}^3 & K_{22}^3 + K_{11}^4 & K_{12}^4 \\ 0 & 0 & 0 & K_{21}^4 & K_{22}^4 \end{bmatrix} \end{matrix} ;$$

$$\{T\} = \begin{Bmatrix} 0 \\ 0 \\ 0 \\ 0 \\ T_t \end{Bmatrix} \begin{matrix} 1 \\ 2 \\ 3 \\ 4 \\ 5 \end{matrix}$$

For completeness, and to facilitate the replication of the results, the global stiffness matrices and joint load vector for $m = 1, 0.8, 0.5$ and 0.2 in Fig. 6(a) are shown below:

$$[K_G]_{m=1} = \begin{bmatrix} 231510.7 & -167730.8 & 0 & 0 & 0 \\ -167730.8 & 508270.2 & -147513.8 & 0 & 0 \\ 0 & -147513.8 & 569967.1 & -26406.4 & 0 \\ 0 & 0 & -26406.4 & 637815.7 & -17874.9 \\ 0 & 0 & 0 & -17874.9 & 344608.1 \end{bmatrix}$$

$$[K_G]_{m=0.8} = \begin{bmatrix} 322037.9 & -242736.7 & 0 & 0 & 0 \\ -242736.7 & 655140.6 & -187359.9 & 0 & 0 \\ 0 & -187359.9 & 643264.6 & -26267.4 & 0 \\ 0 & 0 & -26267.4 & 569484.8 & -10522.4 \\ 0 & 0 & 0 & -10522.4 & 249274.0 \end{bmatrix}$$

$$[K_G]_{m=0.5} = \begin{bmatrix} 580910.5 & -465093.3 & 0 & 0 & 0 \\ -465093.3 & 1050739.4 & -289266.4 & 0 & 0 \\ 0 & -289266.4 & 814645.4 & -25251.3 & 0 \\ 0 & 0 & -25251.3 & 449192.7 & -2730.0 \\ 0 & 0 & 0 & -2730.0 & 111663.7 \end{bmatrix}$$

$$[K_G]_{m=0.2} = \begin{bmatrix} 1215822.3 & -1033168.3 & 0 & 0 & 0 \\ -1033168.3 & 1958404.8 & -505569.4 & 0 & 0 \\ 0 & -505569.4 & 1139292.3 & -22073.1 & 0 \\ 0 & 0 & -22073.1 & 305398.9 & -77.9 \\ 0 & 0 & 0 & -77.9 & 15283.7 \end{bmatrix}$$

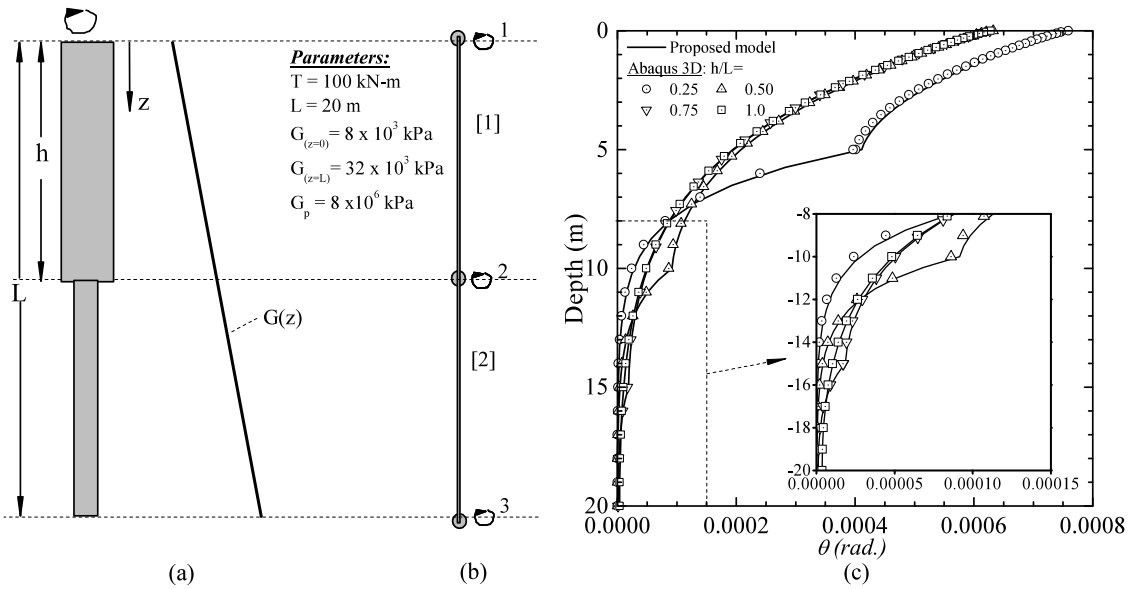

Fig. 7. Example 4: (a) Stepped pile in a one-layered non-homogeneous soil, (b) segment numbering and degrees of freedom and (c) angles of twist profile for $h/L = 0.25$, $h/L = 0.5$, $h/L = 0.75$ and $h/L = 1.0$.

and

$$\{T\} = \{0 \quad 0 \quad 0 \quad 0 \quad 100\}^T$$

The nodal angles of twist in global coordinates, $\{\theta\} = \{\theta_1, \theta_2, \theta_3, \theta_4, \theta_5\}^T$, for $m = 1, 0.8, 0.5$ and 0.2 were obtained by solving $\{\theta\} = [K_G]^{-1}\{T\}$. They are:

$$\{\theta\}_{m=1.0} = 10^{-3} \cdot \{0.58256,\ 0.20789,\ 0.05390,\ 0.00223,\ 0.00011\}^T$$
$$\{\theta\}_{m=0.8} = 10^{-3} \cdot \{0.44660,\ 0.18053,\ 0.05268,\ 0.00243,\ 0.00010\}^T$$
$$\{\theta\}_{m=0.5} = 10^{-3} \cdot \{0.28352,\ 0.13912,\ 0.04948,\ 0.00278,\ 0.00011\}^T$$
$$\{\theta\}_{m=0.2} = 10^{-3} \cdot \{0.16662,\ 0.09929,\ 0.04412,\ 0.00319,\ 0.00002\}^T$$

Once the nodal angles of twist vector in global coordinates were known, the end-torques on the individual element were calculated with the element local stiffness matrix $[K]_i$ and local angles of twist $\{\theta\}_i$ as $\{T\}_i = [K]_i\{\theta\}_i$ (i.e., i=1, 2, 3 and 4). Figs. 6(a) and (b) show the angles of twist profiles for the two cases discussed herein. These profiles were obtained from Eqs. (6) and (9); where, for each segment, the first coefficients of the $\{\theta\}_i$ and $\{T\}_i$ vectors are $\bar{\theta}(0)$ and T_a, respectively. $\bar{\theta}(2) - \bar{\theta}(m)$ were determined from the recursive equation (Eq. (8)). The results from the proposed formulation are in excellent agreement with those obtained from Abaqus 3D and those reported by Misra et al. [21] for the case of $m = 1$.

6.4. Example 4: Stepped pile in a one-layered non-homogeneous soil

Fig. 7 shows the angle of twist profile for a stepped pile in a one-layered non-homogeneous soil. The pile has a total length of 20 m and is subjected at its head to a torsional load of 100 kN-m. The shear modulus of the soil $G(z)$ is assumed to vary linearly with depth as shown in Fig. 7(a). $G(z)$ at the surface is $G_{z=0} = 8 \cdot 10^3$ kPa and at the pile toe $G_{z=L_p} = 32 \cdot 10^3$ kPa. The shear modulus of the pile is taken as $G_p = 8 \cdot 10^6$ kPa. The upper portion of the stepped pile has a length h and a radius $r = 0.5$ m. The lower portion of the pile has a length $L - h$ and a radius $r = 0.25$ m. The analysis was performed for four h/L ratios (i.e., $h/L = 0.25$, 0.5, 0.75 and 1.0).

For the analysis, the stepped pile was subdivided into two segments. The first segment was assigned to the upper portion of the pile and the second one to the lower portion. Fig. 7(b) shows the segment numbering and global degrees of freedom at the joints. Fig. 7(c) shows the angle of twist profiles and their comparisons with those obtained from Abaqus 3D. The results between the proposed method and those from Abaqus 3D are in excellent agreement.

6.5. Example 5: Pile partially embedded in a two-layered soil

The capabilities of the proposed approach to accurately capture, in a simple and practical manner, the torsional response of partially embedded piles in multi-layered soils is demonstrated in this example. Fig. 8 shows the angle of twist profile for a prismatic, tapered and stepped pile partially embedded in a two-layered soil deposit. For the stepped pile, it is assumed that the bottom end of the upper portion of the pile coincides with the layer–layer interface. Each pile (i) has a total length of 23 m, of which 3 m are unembedded as depicted in Fig. 8(a) and (ii) is subjected at its head and at the surface level to torsional loads of 50 kN-m and 200 kN-m, respectively. It is assumed that (i) the thickness of the upper and lower layers are h and $L - h$, respectively, (ii) in the upper and lower layers, $G(z)$ is uniformly distributed and has a magnitude of G_1 and $G_2 = 8 \cdot 10^3$ kPa, respectively, and (iii) the shear modulus of the pile is $G_p = 8 \cdot 10^6$ kPa. The analysis is performed for two values of h/L ratios and two values of G_1/G_2 (i.e., $h/L = 0.25$, $h/L = 0.75$, G_1/G_2=0.25 and G_1/G_2=4).

Following the same procedure as that described in previous examples, the analysis was conducted by dividing the pile at the layer–layer and layer–air interfaces (i.e., into three segments). Fig. 8(b) shows the segment numeration and global degrees of freedom. For the unembedded portion of the pile, the shear modulus of the soil was taken as $G(z) = 0$ (i.e., $G_o = s = t = 0$). Figs. 8(c) to (e) show the angle of twist profiles and their comparisons with those obtained from Abaqus 3D for the stepped, tapered and prismatic pile, respectively. Fig. 8 shows a good agreement between the results from the proposed method and those obtained from Abaqus 3D. The maximum relative difference in θ is between 7% and 8% and it occurs to the prismatic element for values of $G_1/G_2 = 0.25$. This difference could be attributed to the load transfer mechanism associated with each method in combination with the higher shear stresses transferred from the pile to the upper portion of the soil (due to a smaller cross-section). As discussed by Nghiem and Chang [22], the torque applied at the pile head travels in the vertical direction and then is transmitted to the soil in the form of radial and vertical shear stresses. The proposed model does not account for the effect of the vertical shear stress. Abaqus 3D uses a more robust constitutive model that accounts for the distribution of the shear stresses in both directions.

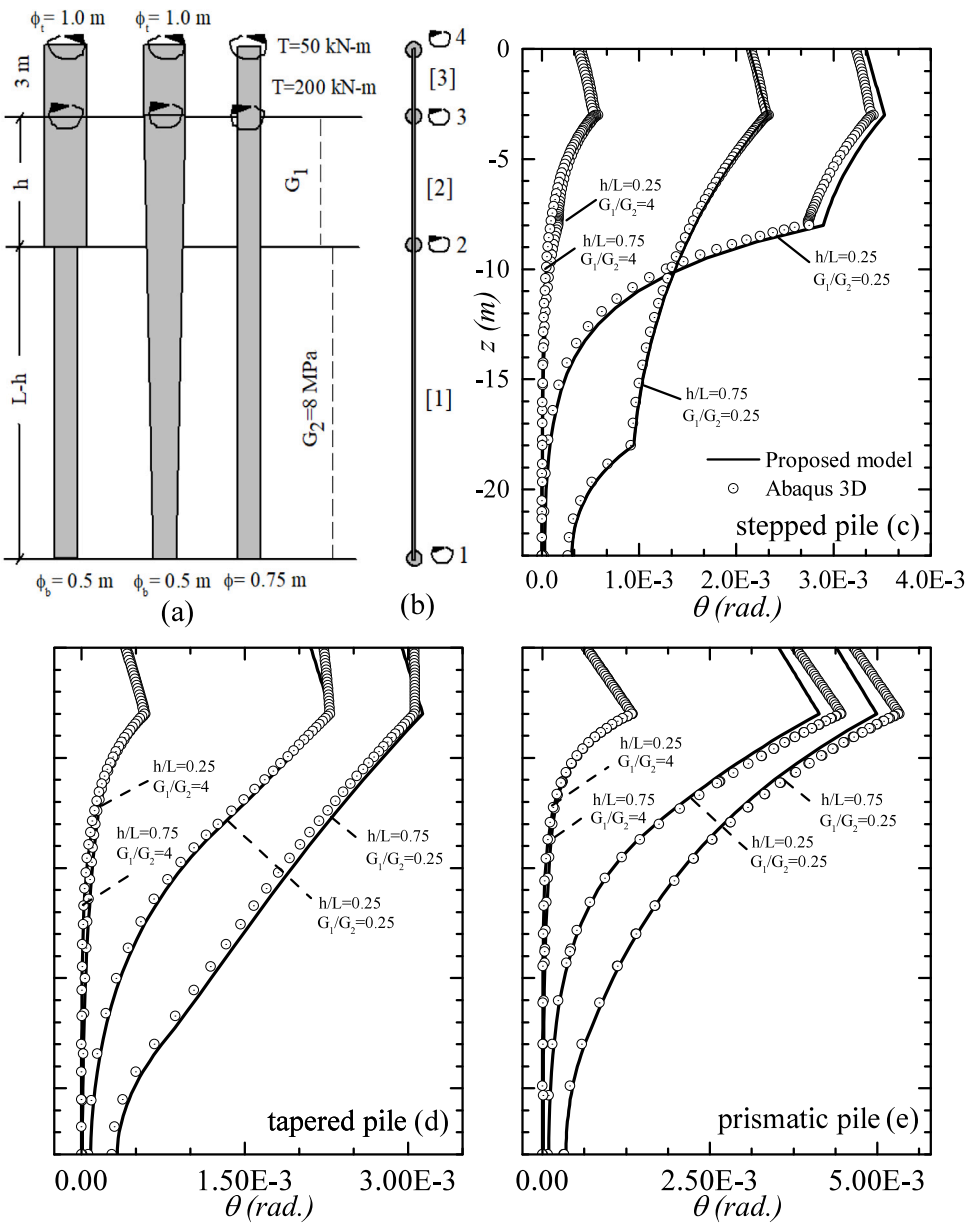

Fig. 8. Example 5: Partially embedded pile in a two-layered soil (a) structural model, (b) segment numbering and global degrees of freedom, (c) θ for stepped pile, (d) θ for tapered pile and (e) θ for prismatic pile.

7. Conclusions

A new matrix method to investigate the torsional response of non-uniform circular piles in multi-layered non-homogeneous elastic soils was derived and presented in detail. The analysis of prismatic, tapered and stepped piles partially or fully embedded in multi-layered soils can be easily conducted in a simple manner with the proposed formulation - a difficult and cumbersome endeavor when using available analytical and numerical methods. The matrix formulation proposed herein can be easily implemented into already available structural matrix analysis codes. The proposed method is of great practical interest to practitioners, who lack of simple and accurate models to analyze complex problems of torsionally loaded piles.

The stiffness matrix of a single pile segment was derived and then used to investigate, by means of classical matrix methods of structural analysis, the torsional response of piles in multi-layered soils. The shear modulus distribution along each segment of pile was assumed to fit a quadratic function, so a wide range of soil conditions can be accounted for. Eight simple steps were provided to study the overall torsional response of short piles in a one-layered soil while accounting for the contribution of the torsional stiffness at the pile base. The analysis of piles embedded in soils made up of multiple layers was carried out by dividing the pile into multiple segments, each segment representing a change in soil properties or pile geometry. Five examples were presented to validate the simplicity and practicality of the proposed method to accurately capture the torsional response of piles in multi-layered soils. The results from the proposed method were found to be in excellent agreement with those obtained from the finite element analysis package Abaqus 3D and more cumbersome analytical and numerical approaches.

Declaration of competing interest

The authors declare that they have no known competing financial interests or personal relationships that could have appeared to influence the work reported in this paper.

Acknowledgments

This research was carried out at the University of Antioquia, Medellín, Colombia. The support of the Infrastructure Research Group (GII) of the University of Antioquia is appreciated. The author is thankful to Camilo Jose Fernandez-Escobar, Civil and Environmental Engineering undergraduate student at the University of Antioquia, for his help in running examples in Abaqus 3D.

Appendix

Transformation of the GDE into a recursive equation

Eq. (5) can be rewritten as follows:

$$J(\zeta)\frac{d^2\theta}{d\zeta^2} + \frac{d\theta}{d\zeta}\frac{dJ}{d\zeta} = \frac{L^2}{G_p}R(\zeta)\theta(\zeta) \tag{A.1}$$

Using property # 4 from Table 2, the following transformed functions for terms of the GDE are obtained:

$$J(\zeta)\frac{d^2\theta}{d\zeta^2} = \sum_{r=0}^{k}\bar{J}(k-r)(r+1)(r+2)\bar{\theta}(r+2) \tag{A.2}$$

$$R(\zeta)\theta(\zeta) = \sum_{r=0}^{k}\bar{R}(k-r)\bar{\theta}(r) \tag{A.3}$$

$$\frac{d\theta}{d\zeta}\frac{dJ}{d\zeta} == \sum_{r=0}^{k}(k-r+1)\bar{J}(k-r+1)(r+1)\bar{\theta}(r+1) \tag{A.4}$$

From the kronecker delta function from Table 2 (property # 5), one knows that:

$$\begin{aligned}
&\bar{J}(k) = S_o\delta(k) + S_1\delta(k-1) + S_2\delta(k-2) + S_3\delta(k-3) + S_4\delta(k-4) \\
&\bar{J}(k-r) = S_o\delta(k-r) + S_1\delta(k-r-1) + S_2\delta(k-r-2) \\
&+ S_3\delta(k-r-3) + S_4\delta(k-r-4) \\
&\bar{J}(k-r+1) = S_o\delta(k-r+1) + S_1\delta(k-r) + S_2\delta(k-r-1) \\
&+ S_3\delta(k-r-2) + S_4\delta(k-r-3)
\end{aligned} \tag{A.5}$$

$$\begin{aligned}
&\bar{R}(k) = R_o\delta(k) + R_1\delta(k-1) + R_2\delta(k-2) + R_3\delta(k-3) \\
&+ R_4\delta(k-4) \\
&\bar{R}(k-r) = R_o\delta(k-r) + R_1\delta(k-r-1) + R_2\delta(k-r-2) + R_3\delta(k-r-3) \\
&+ R_4\delta(k-r-4)
\end{aligned} \tag{A.6}$$

Now, substituting Eqs. (A.5) and (A.6) into Eqs. (A.2)–(A.4), and then substituting the resulting expressions into Eq. (A.1), the following equation is obtained:

$$\begin{aligned}
&S_0(k+1)(k+2)\bar{\theta}(k+2) + S_1k(k+1)\bar{\theta}(k+1) + S_2(k-1)k\bar{\theta}(k) \\
&+ S_3(k-2)(k-1)\bar{\theta}(k-1) \\
&+ S_4(k-3)(k-2)\bar{\theta}(k-2) + S_1(k+1)\bar{\theta}(k+1) + 2S_2k\bar{\theta}(k) \\
&+ 3S_3(k-1)\bar{\theta}(k-1) \\
&+ 4S_4(k-2)\bar{\theta}(k-2) \\
&= \frac{L^2}{G_p}\left[R_o\bar{\theta}(k) + R_1\bar{\theta}(k-1) + R_2\bar{\theta}(k-2) + R_3\bar{\theta}(k-3) + R_4\bar{\theta}(k-4)\right]
\end{aligned} \tag{A.7}$$

Finally, solving for $\bar{\theta}(k+2)$ in Eq. (A.7), the recursive form of the GDE is found (Eq. (8)).

References

[1] El Naggar MH, Wei JQ. Response of tapered piles subjected to lateral loading. Can Geotech J 1999;36(1):52–71. http://dx.doi.org/10.1139/t98-094.
[2] El Naggar MH, Wei JQ. Axial capacity of tapered piles established from model tests. Can Geotech J 1999;36(6):1185–94. http://dx.doi.org/10.1139/t99-076.
[3] Sakr M, El Naggar MH, Nehdi M. Lateral behaviour of composite tapered piles in dense sand. Proc Inst Civ Eng Geotech Eng 2005;158(3):145–57. http://dx.doi.org/10.1680/geng.2005.158.3.145.
[4] Kamran Khan M, El Naggar MH, Elkasabgy M. Compression testing and analysis of drilled concrete tapered piles in cohesive-frictional soil. Can Geotech J 2008;45(3):377–92. http://dx.doi.org/10.1139/T07-107.
[5] Liu J, Shao X, Cheng B, Cao G, Li K. Study on buckling behavior of tapered friction piles in soft soils with linear shaft friction. Adv Civ Eng 2020;2020. http://dx.doi.org/10.1155/2020/8865656.
[6] Singh S, Patra NR. Axial behavior of tapered piles using cavity expansion theory. Acta Geotech 2020;15(6):1619–36. http://dx.doi.org/10.1007/s11440-019-00866-y.
[7] Ghazavi M, Tavasoli O. Characteristics of non-uniform cross-section piles in drivability. Soil Dyn Earthq Eng 2012;43:287–99. http://dx.doi.org/10.1016/j.soildyn.2012.07.017.
[8] Tavasoli O, Ghazavi M. Effect of tapered and semi-tapered geometry on the offshore piles driving performance. Ocean Eng 2020;201. http://dx.doi.org/10.1016/j.oceaneng.2020.107147.
[9] Poulos HG. Torsional response of piles. J Geotech Eng Div 1975;101(10):1019–35.
[10] Randolph MF. Piles subjected to torsion. J Geotech Eng Div 1981;107(8):1095–111. http://dx.doi.org/10.1061/ajgeb6.0001177.
[11] Karasudhi P, Rajapakse RK, Hwang BY. Torsion of a long cylindrical elastic bar partially embedded in a layered elastic half space. Int J Solids Struct 1984;20(1):1–11. http://dx.doi.org/10.1016/0020-7683(84)90071-4.
[12] Chow YK. Torsional response of piles in nonhomogeneous soil. J Geotech Eng 1985;111(7):942–7. http://dx.doi.org/10.1061/(ASCE)0733-9410(1985)111:7(942).
[13] Hache RA, Valsangkar AJ. Torsional resistance of single pile in layered soil. J Geotech Eng 1988;114(2):216–20. http://dx.doi.org/10.1061/(ASCE)0733-9410(1988)114:2(216).
[14] Rajapakse RK. A torsion load transfer problem for a class of non-homogeneous elastic solids. Int J Solids Struct 1988;24(2):139–51. http://dx.doi.org/10.1016/0020-7683(88)90025-X.
[15] Guo WD, Randolph MF. Torsional piles in non-homogeneous media. Comput Geotech 1996;19(4):265–87. http://dx.doi.org/10.1016/S0266-352X(96)00009-2.
[16] Guo WD, Chow YK, Randolph MF. Torsional piles in two-layered nonhomogeneous soil. Int J Geomech 2007;7(6):410–22. http://dx.doi.org/10.1061/(ASCE)1532-3641(2007)7:6(410).
[17] Zhang L. Nonlinear analysis of torsionally loaded piles in a two-layer soil profile. Int J Geomech 2010;10(2):65–73. http://dx.doi.org/10.1061/(asce)gm.1943-5622.0000038.
[18] Zou X, Zhao L, Zhou M, Tian Y. Investigation of the torsional behaviour of circular piles in double-layered nonhomogeneous soil. Appl Ocean Res 2020;98:102110. http://dx.doi.org/10.1016/j.apor.2020.102110.
[19] Rajapakse RKND, Selvadurai APS. Torsional stiffness of non-uniform and hollow rigid piers embedded in isotropic elastic media. Int J Numer Anal Methods Geomech 1985;9(6):525–39. http://dx.doi.org/10.1002/nag.1610090603.
[20] Selvadurai APS, Rajapakse RKND. Variational scheme for analysis of torsion of embedded nonuniform elastic bars. J Eng Mech 1987;113(10):1534–50. http://dx.doi.org/10.1061/(asce)0733-9399(1987)113:10(1534).
[21] Misra A, Saggu R, Basu D, Chakraborty T. Analysis of pile subjected to torsion in multi-layered soil. Int J Numer Anal Methods Geomech 2014;38(5):475–92. http://dx.doi.org/10.1002/nag.2213.
[22] Nghiem HM, Chang NY. Efficient solution for a single pile under torsion. Soils Found 2019;59(1):13–26. http://dx.doi.org/10.1016/j.sandf.2018.08.015.
[23] Vega-Posada CA. Stiffness matrix method for analysis of torsionally loaded piles in multi-layered soils. Proc Inst Civ Eng - Geotech Eng 2022.
[24] Zhou JK. Differential transformation and its applications for electrical circuits. 1986, Huarjung Univ. Press..
[25] Abdel-Halim Hassan IH. Application to differential transformation method for solving systems of differential equations. Appl Math Model 2008;32:2552–9. http://dx.doi.org/10.1016/j.apm.2007.09.025.
[26] Vega-Posada CA, Gallant AP, Areiza-Hurtado M. Simple approach for analysis of beam-column elements on homogeneous and non-homogeneous elastic soil. Eng Struct 2020;221:111110. http://dx.doi.org/10.1016/j.engstruct.2020.111110.
[27] Randolph MF. Piles subjected to torsion. J Geotech Eng Div 1981;107(8):1095–111. http://dx.doi.org/10.1061/ajgeb6.0001177.
[28] Przemieniecki JS. Theory of matrix structural analysis. Dover Publications; 1985, p. 241.
[29] McGuire W, Gallagher RH, Ziemian RD. Matrix structural analysis. second ed.. CreateSpace Independent Publishing; 2015, p. 482.